Comparison of Simulation of Contact Force Control of Flexible Manipulator Using Bernoulli-Euler theory and Timoshenko theory

Minoru Sasaki[a*], Takashi Kuwabara[a], Waweru Njeri[a], Kojiro Matsushita[a] and Harrison Ngetha[b]

[a]Department of Mechanical Engineering, Faculty of Engineering,

Gifu University, 1-1 Yanagido, Gifu, 501-1193 Japan.

[b]Department of Electrical & Electronic Engineering, School of Engineering,

Dedan Kimathi University of Technology, P.O. Box 657-10100 Nyeri, Kenya.

*sasaki@gifu-u.ac.jp

Manuscript history: *Received: 17/05/2017; In revised form: 12/12/2018; Accepted: 11/02/2019*

Published: 12/02/2019

Comparison of Simulation of Contact Force Control of Flexible Manipulator Using Bernoulli-Euler theory and Timoshenko theory

---

Abstract

DOI: 10.33803/JASETD.2017.3-2.2

Industrial robots are expected to be used in circumstances where they can be directly touched by humans like the welfare robot which assists the elderly in the society. Considering the nature of this application in terms of safety, the control of the contact force becomes a requirement along with the conventional control of position. In this article, simulation of the contact force control of a flexible manipulator to investigate the influence of shear deformation and rotational inertia, which varies depending on the sectional shape of a beam, on the result between the Bernoulli-Euler beam theory and Timoshenko beam theory. Comparisons are presented without considering shear deformation and rotational inertia and considering its effectiveness.

Keywords: Bernoulli-Euler, Timoshenko, Contact force control

1. INTRODUCTION

In the recent past, robots are used in various places as a tool to replace the human in undertaking daily chores. For example, in production centers, they are used in various applications such as assembly robots, mobile robots, painting robots, inspection robots etc. Also in our day to day live there are examples of utilization such as nursing care robots, welfare robots, etc, which are needed in the future aging society. For use as a nursing robot or a welfare robot, higher standards of safety are required since it is used in an environment where they are in direct contact with humans. Therefore, in addition to the position control (Shimizumi Yoshimi, 2008) of the robot arm that has been done so far, it is important to control the contact force at the same time.

To investigate the control of the contact force and its dependence on the shear deformation and the rotational inertia which in turn depend on the cross-section of the beam, simulations of the flexible manipulator were carried out using Bernoulli-Euler and Timoshenko beam theories (Endo Takahiro, 2013; Minoru Sasaki K. N., 2015; Takahiro Endo M. S., 2017; Takahiro Endo M. S., 2017). For Bernoulli-Euler beam theory, we neglected the effect of shear deformation and rotational inertia. Timoshenko beam theory considers rotational inertia, however, in this article, we consider the range where this influence can be neglected [2]. We also compared the control models within the range where the influence is negligible and verified the mechanisms.

The contact force control simulation (Shimizumi Yoshimi, 2008)of the link Flexible Timoshenko Arm (Minoru Sasaki K. N., 2015) was numerically simulated using the Fast Inversion Laplace Transform(FILT) algorithm (Hosono, 1984), and the effectiveness of the beam theory.

2. THEORETICAL ANALYSIS

In this section, we present the model to be controlled and derive the equations of motion and boundary conditions of 1-link Flexible Bernoulli-Euler Arm and 1 link Flexible Timoshenko Arm, respectively. The general solutions to be used for simulation are derived using Laplace transformed

$$y(x,t) = w(x,t) - x\theta(t) \tag{2.1}$$

$$\ddot{y}(x,t) + \frac{EI}{\rho} y''''(x,t) = 0 \tag{2.2}$$

equation of motion and boundary condition.

2.1 Theoretical Analysis of Flexible Bernoulli-Euler Arm

A. Link Flexible Bernoulli-Euler Arm model and equation of motion

A model of 1 link Flexible Bernoulli-Euler Arm in this study is shown in Figure 2.1.

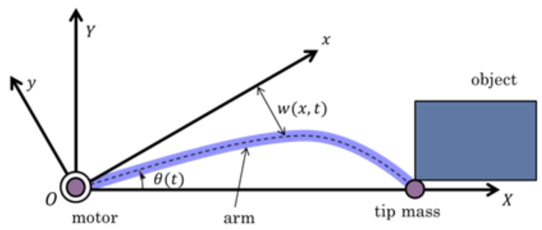

Fig.2.1 Flexible Bernoulli-Euler Arm in contact with an object.

The base of the Flexible Bernoulli-Euler arm has a motor that rotates the arm and rotation can be controlled by the actuator. Also, the tip of the arm is in contact with the object. The arm is of length l, uniform density ρ, secondary moment of area I, Young's modulus E, moment of inertia J of the motor, motor torque τ_a (t), motor rotation angle $\theta(t)$. Furthermore, $w(x,t)$ is the transverse displacement of the point x on the x axis of the arm at a certain time t, the equation of motion of this model can be obtained as follows.

and the boundary condition

$$J\ddot{\theta}(t) = \tau_a(t) - EIw''(0,t) = \tau(t) \tag{2.3}$$

$$y(0,t) = y(l,t) = y''(l,t) = l\theta(t) - w(l,t) = 0 \tag{2.4}$$

The contact force is expressed as follows

$$\lambda(t) = EIw'''(l,t) \tag{2.5}$$

B. Contact force control and boundary control controller

To control the contact force of the tip of the flexible arm, it is necessary to consider boundary control. Denoting the target contact force by λ_d and the target position and angle as $y_d(x)$, θ_d, the following relational expression is obtained.

$$y_d(x) = \frac{\lambda_d}{6EI}x(2l^2 - 3lx + x^2) \tag{2.6}$$

$$\theta_d = -y_d(0) = -\frac{l^2\lambda_d}{3EI} \tag{2.7}$$

The control law is also obtained as follows.

$$\tau(t) = -\tilde{k}_1 EI\{y''(0,t) - y_d''(0)\} - \tilde{k}_2 EI\dot{y}''(0,t) \tag{2.8}$$

($\tilde{k}_1$,$\tilde{k}_2$ are feedback gains.)

C. Preparation of simulation of Flexible Bernoulli-Euler Arm

In simulating the Flexible Bernoulli-Euler Arm of this model, it is necessary to derive a general solution of *w(x, t).* In this section, a general solution of *w(x, t)* is derived using the equation of motion and the boundary condition shown in subsection 2.1.1. The Laplace transform of the equation of motion, the boundary condition, and the control law is as follows.

$$s^2 y(x,s) + \frac{EI}{\rho} y''''(x,s) = 0 \quad (2.9)$$

Solving for *y(x,s)* from equation (2.9) (where F1 (s), F2 (s), F3 (s), F4 (s) are unknowns and *i* is the complex numbers operator)

$$\mathrm{y(x,s)} = \quad (2.10)$$

$$\mathrm{F1(s)e}^{-\frac{\mathrm{i}(-\mathrm{s}^2\mathrm{E}^3\mathrm{I}^3\rho)^{\frac{1}{4}}x}{EI}} + \mathrm{F2(s)e}^{-\frac{(-\mathrm{s}^2\mathrm{E}^3\mathrm{I}^3\rho)^{\frac{1}{4}}x}{EI}} + \mathrm{F3(s)e}^{\frac{\mathrm{i}(-\mathrm{s}^2\mathrm{E}^3\mathrm{I}^3\rho)^{\frac{1}{4}}x}{EI}} + \mathrm{F4(s)e}^{\frac{(-\mathrm{s}^2\mathrm{E}^3\mathrm{I}^3\rho)^{\frac{1}{4}}x}{EI}}$$

$$\mathrm{s}^2\theta(\mathrm{s}) = -\mathrm{k}_1\mathrm{EI}\left\{\mathrm{y}''(0,\mathrm{s}) - \frac{1}{\mathrm{s}}\mathrm{y}''_{\mathrm{d}}(0)\right\} - \mathrm{k}_2\mathrm{sEIy}''(0,\mathrm{s}) \quad (2.11)$$

Where equation (2.11) is Laplace transformed version of (2.3) and $k_1 = \tilde{k}_1/JAs$, $k_2 = \tilde{k}_2/J$.

Substituting (2.6) (2.10) into the equation (2.11) and rearranging

$$\theta(\mathrm{s}) = \frac{-\mathrm{s}(\mathrm{k}_1+\mathrm{sk}_2)\left(-\mathrm{F1(s)}+\mathrm{F2(s)}-\mathrm{F3(s)}+\mathrm{F4(s)}\right)\sqrt{-s^2E^3I^3\rho} - k_1\lambda_d lEI}{EIs^3} \quad (2.12)$$

From (2.10) and (2.12), *w(x,s)* derives

JASETD. ISSN 2309-0936

$$
\begin{aligned}
&\mathrm{w}(\mathrm{x},\mathrm{s}) \\
&= \mathrm{F1}(\mathrm{s})\mathrm{e}^{-\frac{\mathrm{i}(-\mathrm{s}^2\mathrm{E}^3\mathrm{I}^3\rho)^{\frac{1}{4}}x}{EI}} + \mathrm{F2}(\mathrm{s})\mathrm{e}^{-\frac{(-\mathrm{s}^2\mathrm{E}^3\mathrm{I}^3\rho)^{\frac{1}{4}}x}{EI}} + \mathrm{F3}(\mathrm{s})\mathrm{e}^{\frac{\mathrm{i}(-\mathrm{s}^2\mathrm{E}^3\mathrm{I}^3\rho)^{\frac{1}{4}}x}{EI}} + \mathrm{F4}(\mathrm{s})\mathrm{e}^{\frac{(-\mathrm{s}^2\mathrm{E}^3\mathrm{I}^3\rho)^{\frac{1}{4}}x}{EI}} \\
&+ \frac{\mathrm{x}(-\mathrm{s}(\mathrm{k}_1+\mathrm{sk}_2)(-\mathrm{F1}(\mathrm{s})+\mathrm{F2}(\mathrm{s})-\mathrm{F3}(\mathrm{s})+\mathrm{F4}(\mathrm{s}))\sqrt{-s^2E^3I^3\rho}-k_1\lambda_d lEI)}{EIs^3}
\end{aligned} \tag{2.13}
$$

From equation (2.13),

$$
\begin{aligned}
\mathrm{w}'''(\mathrm{l},\mathrm{s}) = \frac{1}{E^3I^3}((-s^2E^3I^3\rho)^{\frac{3}{4}}(IF1(s)\mathrm{e}^{-\frac{\mathrm{i}(-\mathrm{s}^2\mathrm{E}^3\mathrm{I}^3\rho)^{\frac{1}{4}}l}{EI}} - F2(s)\mathrm{e}^{-\frac{(-\mathrm{s}^2\mathrm{E}^3\mathrm{I}^3\rho)^{\frac{1}{4}}l}{EI}} \\
- IF3(s)\mathrm{e}^{-\frac{(-\mathrm{s}^2\mathrm{E}^3\mathrm{I}^3\rho)^{\frac{1}{4}}l}{EI}} + F4(s)\mathrm{e}^{-\frac{(-\mathrm{s}^2\mathrm{E}^3\mathrm{I}^3\rho)^{\frac{1}{4}}l}{EI}}))
\end{aligned} \tag{2.14}
$$

Laplace transforming the expression for the contact force and substituting for $\mathrm{w}'''(\mathrm{l},\mathrm{s})$, rearranging yields

$$
\begin{aligned}
\lambda(\mathrm{s}) = \frac{1}{E^2I^2}((-s^2E^3I^3\rho)^{\frac{3}{4}}(IF1(s)\mathrm{e}^{-\frac{\mathrm{i}(-\mathrm{s}^2\mathrm{E}^3\mathrm{I}^3\rho)^{\frac{1}{4}}l}{EI}} - F2(s)\mathrm{e}^{-\frac{(-\mathrm{s}^2\mathrm{E}^3\mathrm{I}^3\rho)^{\frac{1}{4}}l}{EI}} \\
- IF3(s)\mathrm{e}^{-\frac{(-\mathrm{s}^2\mathrm{E}^3\mathrm{I}^3\rho)^{\frac{1}{4}}l}{EI}} + F4(s)\mathrm{e}^{-\frac{(-\mathrm{s}^2\mathrm{E}^3\mathrm{I}^3\rho)^{\frac{1}{4}}l}{EI}}))
\end{aligned} \tag{2.15}
$$

From (2.15), the system of one link Flexible Bernoulli-Euler Arm can be represented by the block diagram in Figure 2.2.

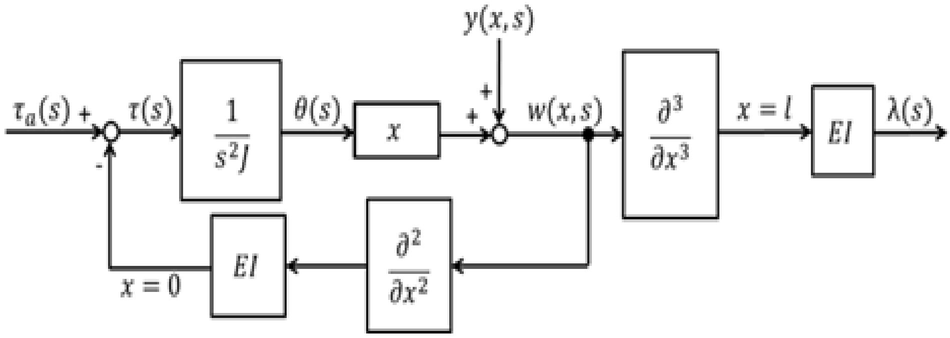

Fig.2.2 Block diagram of 1 link flexible Bernoulli-Euler Arm.

2.2 Theoretical Analysis of Flexible Timoshenko Arm

A. Link Flexible Timoshenko Arm Model and Motion Equation

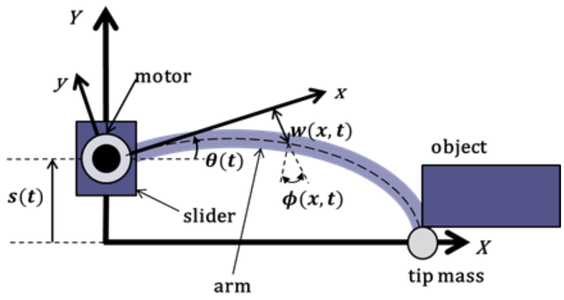

Fig.2.3 Flexible Timoshenko arm in contact with an object.

A 1 link flexible Timoshenko is as shown in Figure 2.3. The base of the flexible armature arm is a motor that rotates the arm and a slider that can slide vertically. Rotation and *y* axis movement can be controlled by the actuator. Also, the tip of the arm is in contact with the object.

The arm is of length *l*, linear density ρ, the moment of inertia $I\rho$, the geometrical moment of inertia *I*, the Young's modulus *E*, the motor's moment of inertia *J*, the motor's torque $\tau_m (t)$ and the motor rotation angle θ). The slider mass is *M*, slider force $F_s (t)$, and height *S(t)*.

Furthermore, let *w(x,t)* be the transverse displacement of the point *x* on the *x* axis of the arm at a certain time *t*, $\varphi(x,t)$ be the rotation angle of the cross section for the x axis and the bending change of the arm. The equations of motion of the model are obtained as follows.

$$\rho\left[\ddot{w}(x,t) + x\ddot{\theta}(t) + \ddot{S}(t)\right] + K[\varphi'(x,t) - w''(x,t)] = 0 \tag{2.16}$$

$$I_{\rho}\left[\ddot{\varphi}(x,t) + \ddot{\theta}(t)\right] + K[\varphi(x,t) - w'(x,t)] - EI\varphi''(x,t) = 0 \tag{2.17}$$

And the boundary conditions

$$w(0,t) = \varphi(0,t) = \varphi'(l,t) = l\theta(t) + w(l,t) + S(t) = 0 \tag{2.18}$$

$$J\ddot{\theta}(t) = \tau_m(t) + EI\varphi'(0,t) \equiv \tau(t) \tag{2.19}$$

$$M\ddot{S}(t) = F_s(t) + Kw'(0,t) \equiv F(t) \tag{2.20}$$

The contact force is expressed as follows

$$\lambda(t) = K[w'(l,t) - \phi(l,t)] \tag{2.21}$$

B. Contact force control and boundary control controller

C. To control the contact force of the tip of the flexible arm, it is necessary to consider boundary control. Here, when the target contact force is denoted by λ_d and the target values are expressed as $w_d(x)$, $\varphi_d(x)$, θ_d, S_d, the following relational expression is obtained.

$$\begin{cases} \phi_d(x) = \frac{\lambda_d x}{EI}(l - \frac{x}{2}) \\ w_d(x) = \lambda_d x(\frac{1}{K} + \frac{lx}{2EI} - \frac{x^2}{6EI}) \\ l\theta_d + S_d = -\lambda_d l(\frac{1}{K} + \frac{l^2}{3EI}) \end{cases} \tag{2.22}$$

The control law is also obtained as follows.

$$F(t) = \tilde{k}_1 K[w'(0,t) - w_d'(0)] + \tilde{k}_2 K\dot{w}'(0,t) - \tilde{k}_3[S(t) - S_d] - \tilde{k}_4\dot{S}(t) \quad (2.23)$$

$$\tau(t) = \tilde{k}_5 EI[\phi'(0,t) - \phi_d'(0)] + \tilde{k}_6 EI\dot{\phi}'(0,t) - \tilde{k}_7[\theta(t) - \theta_d] - \tilde{k}_8\dot{\theta}(t) \quad (2.24)$$

$\tilde{k}_1$~$\tilde{k}_8$ are feedback gains, (2.23) is the slider control law, and (2.24) is the motor control law.

D. Preparation of simulation of Flexible Timoshenko Arm

In simulating Flexible Timoshenko Arm of this model, it is necessary to derive a general solution of *w(x, t)*, *φ(x, t)*. In this section, general solutions of *w(x, t)* and *φ(x, t)* are derived using the motion equations and boundary conditions shown in Section 2.1.2. Laplace transform of the equations of motion leads to the following.

$$s^2\rho w(x,s) + K\big(\phi'(x,s)\big) - K\big(w''(x,s)\big) + s^2\rho\big(x\theta(s) + S(s)\big) = 0 \quad (2.25)$$

$$\big(s^2 I_\rho + K\big)\phi(x,s) - Kw'(x,s) - EI\phi''(x,s) + s^2 I_\rho\theta(s) = 0 \quad (2.26)$$

Solving the simultaneous differential equations of equations (2.25) and (2.26)(Where F1 (s), F2 (s), F3 (s), F4 (s) are unknowns)

$$\varphi(x,s) = -\theta(s) + F1(s)e^{-\frac{1}{2}\frac{\sqrt{2}\sqrt{KEI\left(s\rho EI+KsI_\rho-\sqrt{s^2\rho^2E^2I^2-2s^2\rho EIKI_\rho+K^2s^2{I_\rho}^2-4K^2EI\rho}\right)}sx}{KEI}}$$
$$+ F2(s)e^{\frac{1}{2}\frac{\sqrt{2}\sqrt{KEI\left(s\rho EI+KsI_\rho-\sqrt{s^2\rho^2E^2I^2-2s^2\rho EIKI_\rho+K^2s^2{I_\rho}^2-4K^2EI\rho}\right)}sx}{KEI}}$$
$$+ F3(s)e^{-\frac{1}{2}\frac{\sqrt{2}\sqrt{KEI\left(s\rho EI+KsI_\rho-\sqrt{s^2\rho^2E^2I^2-2s^2\rho EIKI_\rho+K^2s^2{I_\rho}^2-4K^2EI\rho}\right)}sx}{KEI}} \quad (2.27)$$
$$+ F4(s)e^{\frac{1}{2}\frac{\sqrt{2}\sqrt{KEI\left(s\rho EI+KsI_\rho-\sqrt{s^2\rho^2E^2I^2-2s^2\rho EIKI_\rho+K^2s^2{I_\rho}^2-4K^2EI\rho}\right)}sx}{KEI}}$$

$$w(x,s)$$
$$= \frac{1}{4}\frac{1}{EIsK^2\rho}(\sqrt{KEI\left(s\rho EI+KsI_\rho-\sqrt{s^2\rho^2E^2I^2-4KE\rho\left(\frac{1}{2}s^2I_\rho+K\right)I+K^2s^2{I_\rho}^2}\right)}$$
$$\times\sqrt{2}\,F1(s)\left(-\sqrt{s^2\rho^2E^2I^2-4KE\rho\left(\frac{1}{2}s^2I_\rho+K\right)I+K^2s^2{I_\rho}^2}+\left(\rho EI-I_\rho K\right)s\right)$$
$$\times e^{-\frac{1}{2}\frac{\sqrt{2}\sqrt{KEI\left(s\rho EI+KsI_\rho-\sqrt{s^2\rho^2E^2I^2-4KE\rho\left(\frac{1}{2}s^2I_\rho+K\right)I+K^2s^2{I_\rho}^2}\right)}sx}{KEI}}$$

$$-F2(s)\sqrt{KEI\left(s\rho EI+KsI_\rho-\sqrt{s^2\rho^2E^2I^2-4KE\rho\left(\frac{1}{2}s^2I_\rho+K\right)I+K^2s^2{I_\rho}^2}\right)s}$$

$$\times\sqrt{2}\left(-\sqrt{s^2\rho^2E^2I^2-4KE\rho\left(\frac{1}{2}s^2I_\rho+K\right)I+K^2s^2{I_\rho}^2}+\left(\rho EI-I_\rho K\right)s\right)$$

$$\times e^{\frac{1}{2}\frac{\sqrt{2}\sqrt{KEI\left(s\rho EI+KsI_\rho-\sqrt{s^2\rho^2E^2I^2-4KE\rho\left(\frac{1}{2}s^2I_\rho+K\right)I+K^2s^2{I_\rho}^2}\right)s}x}{KEI}}$$

$$+\left(\sqrt{s^2\rho^2E^2I^2-4KE\rho\left(\frac{1}{2}s^2I_\rho+K\right)I+K^2s^2{I_\rho}^2}+\left(\rho EI-I_\rho K\right)s\right)$$

$$\times F3(s)\sqrt{KEI\left(s\rho EI+KsI_\rho+\sqrt{s^2\rho^2E^2I^2-4KE\rho\left(\frac{1}{2}s^2I_\rho+K\right)I+K^2s^2{I_\rho}^2}\right)s}$$

$$\times\sqrt{2}e^{-\frac{1}{2}\frac{\sqrt{2}\sqrt{KEI\left(s\rho EI+KsI_\rho+\sqrt{s^2\rho^2E^2I^2-4KE\rho\left(\frac{1}{2}s^2I_\rho+K\right)I+K^2s^2{I_\rho}^2}\right)s}x}{KEI}}$$

$$-\left(\sqrt{s^2\rho^2E^2I^2-4KE\rho\left(\frac{1}{2}s^2I_\rho+K\right)I+K^2s^2{I_\rho}^2}+\left(\rho EI-I_\rho K\right)s\right)$$

$$\times F4(s)\sqrt{KEI\left(s\rho EI+KsI_\rho+\sqrt{s^2\rho^2E^2I^2-4KE\rho\left(\frac{1}{2}s^2I_\rho+K\right)I+K^2s^2{I_\rho}^2}\right)s} \qquad (2.28)$$

$$\times\sqrt{2}e^{\frac{1}{2}\frac{\sqrt{2}\sqrt{KEI\left(s\rho EI+KsI_\rho+\sqrt{s^2\rho^2E^2I^2-4KE\rho\left(\frac{1}{2}s^2I_\rho+K\right)I+K^2s^2{I_\rho}^2}\right)s}x}{KEI}}-4K^2Es\rho I(x\theta(s)$$

$$+S(s)))$$

Next, when the boundary conditions is Laplace transformed, they become

$$w(0,s)=0 \qquad (2.29)$$

$$\phi(0,s) = 0 \tag{2.30}$$

$$\phi'(l,s) = 0 \tag{2.31}$$

$$l\theta(s) + w(l,s) + S(s) = 0 \tag{2.32}$$

$$s^2 J\theta(s) = \tau_m(s) + EI\phi'(0,s) \equiv \tau(s) \tag{2.33}$$

$$s^2 MS(s) = F_s(s) + Kw'(0,s) \equiv F(s) \qquad (2.34$$

From this boundary condition, an operation to derive four equations for obtaining the unknowns F1 (s), F2 (s), F3 (s), F4 (s) is performed. First, Laplace transform the equations (2.23) and (2.24)

$$F(s) = \left(\tilde{k}_1 + s\tilde{k}_2\right)Kw'(0,s) - \left(\tilde{k}_3 + s\tilde{k}_4\right)S(s) - \frac{1}{s}\left(\tilde{k}_1 K w_d{}'(0) + \tilde{k}_3 S_d\right) \tag{2.35}$$

$$\tau(s) = \left(\tilde{k}_5 + s\tilde{k}_6\right)EI\phi'(0,s) - \left(\tilde{k}_7 + s\tilde{k}_8\right)\theta(s) - \frac{1}{s}\left(\tilde{k}_5 EI\phi_d'(0) - \tilde{k}_7\theta_d\right) \tag{2.36}$$

Solving for $w'(0, s)$, $\varphi'(0, s)$, $w_d'(0)$, $\varphi_d'(0)$ in the expression (2.35) and (2.36) by differentiating (2.27) and (2.28) are differentiated with respect to x to yield

$$
\begin{aligned}
w'(0,s) = \frac{1}{4}\frac{1}{K^2Es\rho I}(-\Bigg(& s\rho EI + KsI_\rho \\
& - \sqrt{s^2\rho^2E^2I^2 - 2s^2\rho EIKI_\rho + K^2s^2{I_\rho}^2 - 4K^2EI\rho}\Bigg)\mathrm{s} \\
& \times F1(\mathrm{s})(-\sqrt{s^2\rho^2E^2I^2 - 2s^2\rho EIKI_\rho + K^2s^2{I_\rho}^2 - 4K^2EI\rho} \\
& + (EI\rho - I_\rho K)s) \\
& - F2(s)\Bigg(s\rho EI + KsI_\rho \\
& - \sqrt{s^2\rho^2E^2I^2 - 2s^2\rho EIKI_\rho + K^2s^2{I_\rho}^2 - 4K^2EI\rho}\Bigg) \\
& \times \mathrm{s}(-\sqrt{s^2\rho^2E^2I^2 - 2s^2\rho EIKI_\rho + K^2s^2{I_\rho}^2 - 4K^2EI\rho} \\
& + (EI\rho - I_\rho K)s) \\
& - (\sqrt{s^2\rho^2E^2I^2 - 2s^2\rho EIKI_\rho + K^2s^2{I_\rho}^2 - 4K^2EI\rho} \\
& + (EI\rho - I_\rho K)s) \\
& \times F3(s)\Bigg(s\rho EI + KsI_\rho \\
& + \sqrt{s^2\rho^2E^2I^2 - 2s^2\rho EIKI_\rho + K^2s^2{I_\rho}^2 - 4K^2EI\rho}\Bigg)\mathrm{s} \\
& - (\sqrt{s^2\rho^2E^2I^2 - 2s^2\rho EIKI_\rho + K^2s^2{I_\rho}^2 - 4K^2EI\rho} \\
& + (EI\rho - I_\rho K)s) \\
& \times F4(s)\Bigg(s\rho EI + KsI_\rho \\
& + \sqrt{s^2\rho^2E^2I^2 - 2s^2\rho EIKI_\rho + K^2s^2{I_\rho}^2 - 4K^2EI\rho}\Bigg)\mathrm{s} \\
& - 4K^2Es\rho I\theta(s)
\end{aligned}
\tag{2.37}
$$

$$\varphi'(0,s)$$

$$= -\frac{1}{2}\frac{F1(s)\sqrt{2}\sqrt{KEI\left(s\rho EI + KsI_\rho - \sqrt{s^2\rho^2E^2I^2 - 2s^2\rho EIKI_\rho + K^2s^2{I_\rho}^2 - 4K^2EI\rho}\right)s}}{KEI}$$

$$+\frac{1}{2}\frac{F2(s)\sqrt{2}\sqrt{KEI\left(s\rho EI + KsI_\rho - \sqrt{s^2\rho^2E^2I^2 - 2s^2\rho EIKI_\rho + K^2s^2{I_\rho}^2 - 4K^2EI\rho}\right)s}}{KEI}$$

$$-\frac{1}{2}\frac{F3(s)\sqrt{2}\sqrt{KEI\left(s\rho EI + KsI_\rho + \sqrt{s^2\rho^2E^2I^2 - 2s^2\rho EIKI_\rho + K^2s^2{I_\rho}^2 - 4K^2EI\rho}\right)s}}{KEI} \quad (2.38)$$

$$+\frac{1}{2}\frac{F4(s)\sqrt{2}\sqrt{KEI\left(s\rho EI + KsI_\rho + \sqrt{s^2\rho^2E^2I^2 - 2s^2\rho EIKI_\rho + K^2s^2{I_\rho}^2 - 4K^2EI\rho}\right)s}}{KEI}$$

From equation (2.20)

$$w_d(x) = \lambda_d x\left(\frac{1}{K} + \frac{lx}{2EI} - \frac{x^2}{6EI}\right)$$

Then

$$w_d'(0) = \frac{\lambda_d}{K} \quad (2.39)$$

$$\phi_d(x) = \frac{\lambda_d x}{EI}(l - \frac{x}{2})$$

Then

$$\phi_d{}'(0) = \frac{\lambda_d l}{EI} \tag{2.40}$$

Let us say that both sides of (2.33) are *J* and the expression (2.32) is ， $k_i = k_i/M(i = 1\sim4)$， and let $k_i = k_i/M(i = 5\sim8)$

$$s^2\theta(s) = \tau_m(s) + EI\phi'(0,s) \equiv \tau(s)/M \tag{2.41}$$

$$s^2 S(s) = F_s(s) + Kw'(0,s) \equiv F(s)/J \tag{2.42}$$

(2.35), (2.37), (2.39) into (2.41)

$$\begin{aligned} &s^2\theta(s) \\ &= -\frac{1}{2\,K}\ ((k_5 + sk_6) \times \sqrt{2}\big(\,F1(s) - F2(s)\big) \\ &\times \sqrt{KEI\left(s\rho EI + KsI_\rho - \sqrt{s^2\rho^2E^2I^2 - 2s^2\rho EIKI_\rho + K^2s^2{I_\rho}^2 - 4K^2EI\rho}\right)s} \\ &+ \sqrt{KEI\left(s\rho EI + KsI_\rho + \sqrt{s^2\rho^2E^2I^2 - 2s^2\rho EIKI_\rho + K^2s^2{I_\rho}^2 - 4K^2EI\rho}\right)s} \\ &\times \big(F3(s) - F4(s)\big) - (k_7 + sk_8)\theta(s) - \frac{1}{s}(k_5\lambda_d l - k_7\theta_d) \end{aligned} \tag{2.43}$$

(2.36), (2.38), (2.40) into (2.42)

$$
\begin{aligned}
s^2S(s) = \frac{1}{4}\frac{1}{KEs\rho I}&((k_1 + sk_2)(-\Bigg(s\rho EI + KsI_\rho \\
&- \sqrt{s^2\rho^2E^2I^2 - 2s^2\rho EIKI_\rho + K^2s^2{I_\rho}^2 - 4K^2EI\rho}\Bigg)\mathrm{s} \\
&\times F1(s)\Bigg(-\sqrt{s^2\rho^2E^2I^2 - 2s^2\rho EIKI_\rho + K^2s^2{I_\rho}^2 - 4K^2EI\rho} \\
&+ \left(EI\rho - I_\rho K\right)s\Bigg) \\
&- F2(s)\Bigg(s\rho EI + KsI_\rho \\
&- \sqrt{s^2\rho^2E^2I^2 - 2s^2\rho EIKI_\rho + K^2s^2{I_\rho}^2 - 4K^2EI\rho}\Bigg) \\
&\times \mathrm{s}\Bigg(-\sqrt{s^2\rho^2E^2I^2 - 2s^2\rho EIKI_\rho + K^2s^2{I_\rho}^2 - 4K^2EI\rho} \\
&+ \left(EI\rho - I_\rho K\right)s\Bigg) \\
&- \Bigg(\sqrt{s^2\rho^2E^2I^2 - 2s^2\rho EIKI_\rho + K^2s^2{I_\rho}^2 - 4K^2EI\rho} \\
&+ \left(EI\rho - I_\rho K\right)s\Bigg) \\
&\times F3(s)\Bigg(s\rho EI + KsI_\rho \\
&+ \sqrt{s^2\rho^2E^2I^2 - 2s^2\rho EIKI_\rho + K^2s^2{I_\rho}^2 - 4K^2EI\rho}\Bigg)\mathrm{s} \\
- (\sqrt{s^2\rho^2E^2I^2 - 2s^2\rho EIKI_\rho + K^2s^2{I_\rho}^2 - 4K^2EI\rho} &+ \left(EI\rho - I_\rho K\right)s) \\
&\times F4(s)\Bigg(s\rho EI + KsI_\rho \\
&+ \sqrt{s^2\rho^2E^2I^2 - 2s^2\rho EIKI_\rho + K^2s^2{I_\rho}^2 - 4K^2EI\rho}\Bigg)\mathrm{s} \\
&- 4K^2Es\rho I\theta(s) - (k_3 + sk_4)S(s) - \frac{1}{s}(k_1\lambda_d + k_3S_d)
\end{aligned}
\tag{2.44}
$$

Next, solving for *S(s)*, *θ(s)* from the simultaneous equations of (2.43) and (2.44) and substituting into equation (2.32) yields one equation.

Substituting *S(s)* and *θ(s)* into the equation (2.30) yields the following equation.

Next from (2.26), the expression of *w(0,s)* is obtained (2.26) as follows.

$$\mathrm{w}(\mathrm{x},\mathrm{s}) = C1S(s) + C\theta(s), \varphi(x,s) = C2S(s) + C4\theta(s) \qquad (2.45)$$

Similarly, obtaining φ (0, s) from (2.25) and (2.28) results in (2.28) as follows. Equation (2.26) with respect to x and obtaining *φ'(1, s)* (2.29) is as follows. (S), F 2 (s), F 3 (s), F 4 (s) from the simultaneous equations of the formulas (2.41), (2.42), (2.43), and (2.44) , (2.26), it becomes a general solution of *φ(x,s)* and *w(x,s)*.

Based on the above, the system of one link Flexible Timoshenko Arm is shown in the block diagram in Figure 2.4.

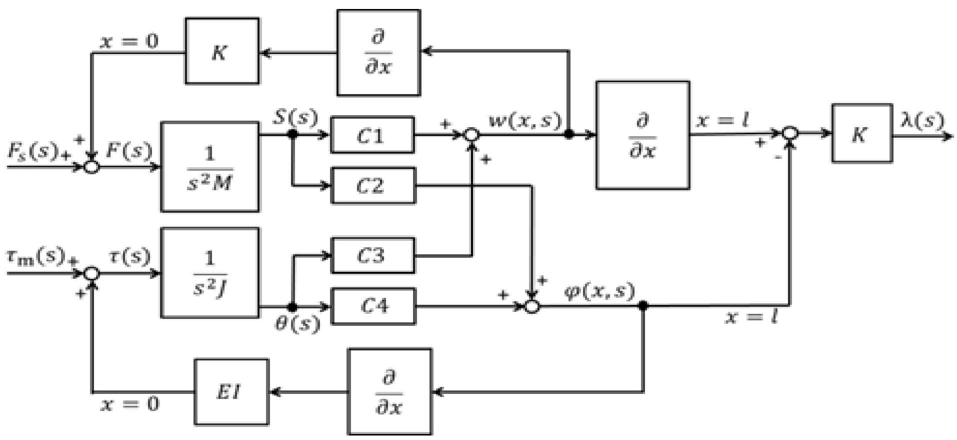

Fig.2.4 Block diagram of 1 link Timoshenko Arm.

3. NUMERICAL SIMULATION

In this section, generalized solution *w(x,s)* based on the FILT algorithm for one link Flexible Bernoulli-Euler Arm derived in the previous section is presented. Flexible Timoshenko Arm *φ(x,s), w(x,s)*, etc. are simulated by performing inverse Laplace transforms. In addition, to make the two models coincide with each other for comparison, $S(t) = 0$ for 1 slider Flexible Timoshenko Arm slider was realized to simulate only the motor operation. Also, since the definition of the deflection distance at the tip of the arm was positive and negative, we negatively compare positive and negative by negating one link Flexible Timoshenko Arm.

To investigate the influence of cross-section on the shear deformation, thickness h and width b of the beam were varied for Bernoulli-Euler beam theory and Timoshenko beam.

3.1 Simulation Parameters

The parameters used in the simulation of this study are shown in Table 3.1. The thickness h and the width b are shown together with the results in Section 3.2.

Table.3.1 System parameters.

Parameter	**Symbol**	**Values**
length	l	1.05[m]
density	ρ_a	7874[kg/m^3]

mass moment of inertia	I_ρ	$2.79x10^{-4}$[kgm]
Young's modulus	E	2.06e11[Pa]
shear modulus	G	7.69e10[Pa]
shear coefficient	κ	3/2
desired contact force	λ_d	-1.0[N]
Desired translational position of the slider	S_d	0.0[m]

Simulation is performed with a beam having a rectangular cross-section, and the distance from the base is x = 1.05 [m].

3.2 Simulation Results

The above parameters are fixed, however, the parameters below change depending on the thickness *h* and the width *b* of the beam:

Cross sectional area $A = bh[m^2]$, geometrical moment of inertia $I = \frac{bh^3}{12}[m^4]$, linear density ρ [kg / m] is derived by $\rho = \rho_a bh$.The comparison is made on the contact force λ (t) when the vibration suppression control law is not set. Inputs when vibration suppression control is not installed are as follows:

1 link Flexible Bernoulli-Euler Arm motor torque $\tau_a(t) = EIy_d''(0)$

1 link Flexible Timoshenko Arm motor torque $\tau_{\mathrm{m}}(t) = -\phi_d'(0)$

The resonance frequency of the waveform as read from the Bode diagram are shown in Fig.3.1 and an error rate is introduced in order to quantitatively compare the deviation in each order. An error occurs when the error rate exceeds 0.5%. While comparing simulations relatively for various thicknesses and widths, we found several features.

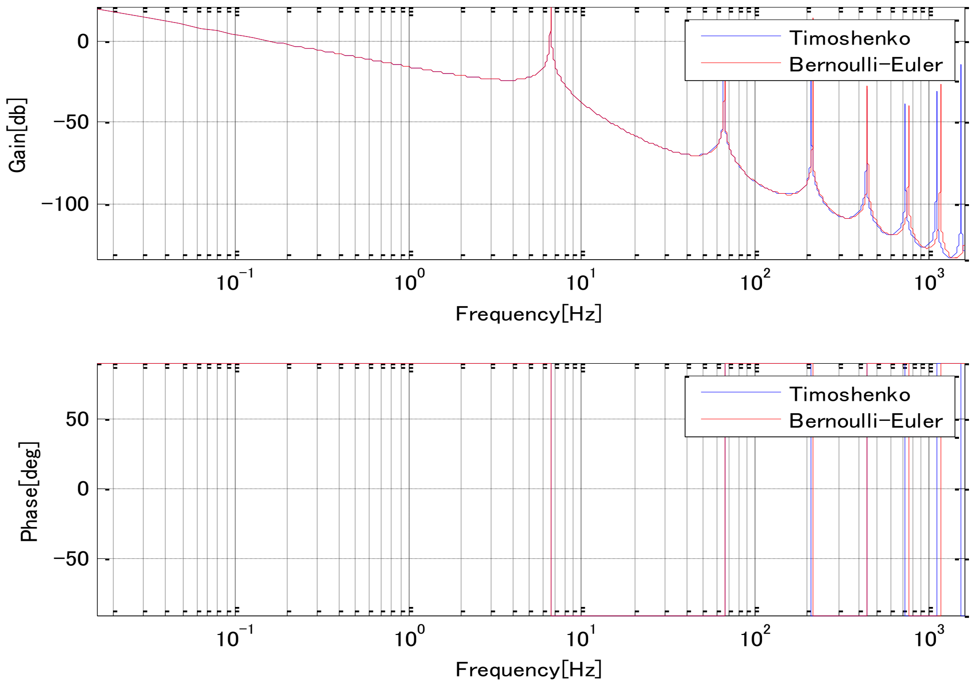

Fig.3.1 Bode diagram of the contact force.

One link Flexible Bernoulli-Euler Arm in Fig.2.1 has no slider mechanism, and it operates only with a motor. On the other hand, the one link Flexible Timoshenko Arm shown in Fig. 2.3 operates with a slider mechanism and a motor. Comparing simulation results of time response with two models, we examine how the slider mechanism will affect the control of the contact force.

Since the cross-section of the beam used in this study has thickness h = 0.02 [m] and width w = 0.00447 [m]. Condition 2 considered in Section 3.3, it is considered that there is almost no influence on the result due to the difference in beam theory.

Other parameters are set in Table 3.1.

On the vibration suppression control law. 1 link Flexible Bernoulli-Euler Arm is the formula (2.8), and the feedback gains are k_1 = 1.2, k_2 = 0.5. One link Flexible Timoshenko Arm is given by the equations (2.32) and (2.33), and the feedback gains are $\tilde{k}_1 = \tilde{k}_5 = 1, \tilde{k}_2 = \tilde{k}_6 = 0.2,\ \tilde{k}_3 = \tilde{k}_7 = 16, \tilde{k}_4 = \tilde{k}_8 = 8$ of the tip of the arm is performed.

The results of each model are shown below.

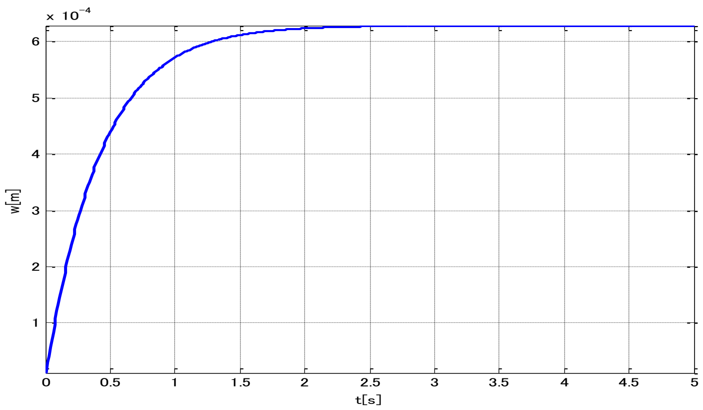

Fig.3.12 Time response of transverse displacement of Bernoulli-Euler arm.

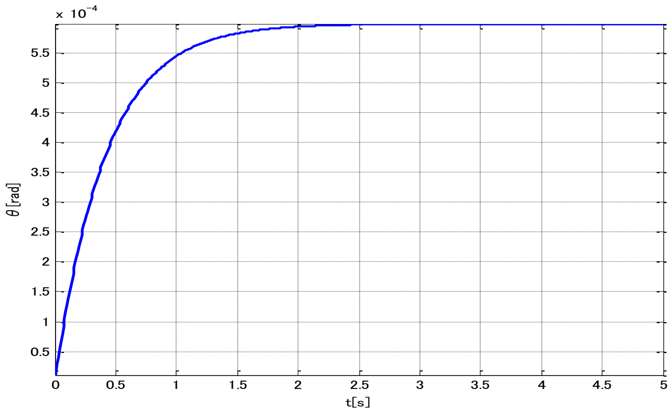

Fig.3.13 Time response of rotational angle.

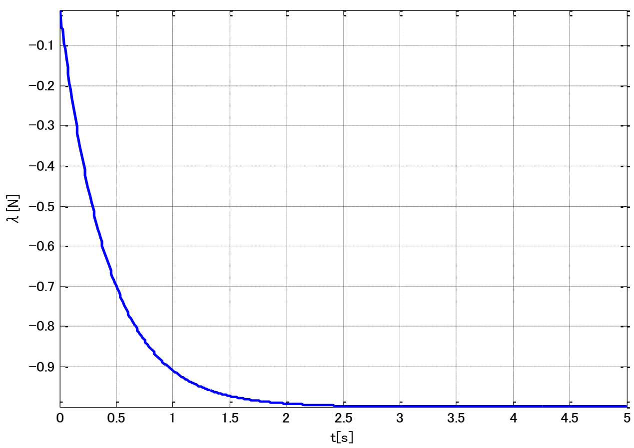

Fig.3.14 Time response of the contact force.

Time response simulation results of 1 link flexible triangular arms.

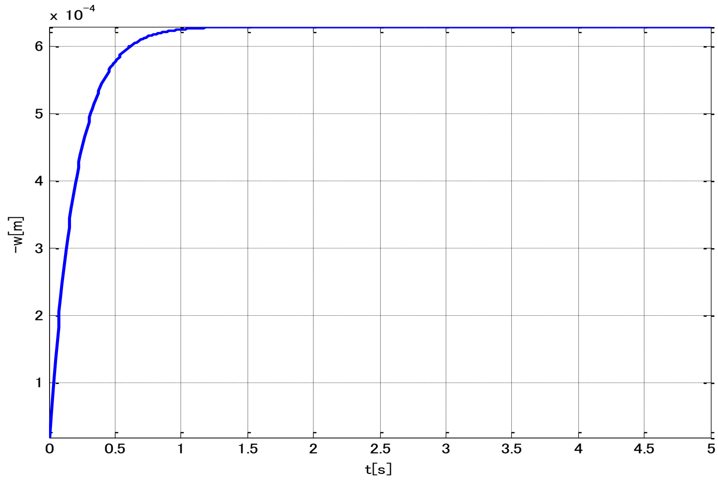

Fig.3.15 Time response of transverse displacement of Timoshenko arm.

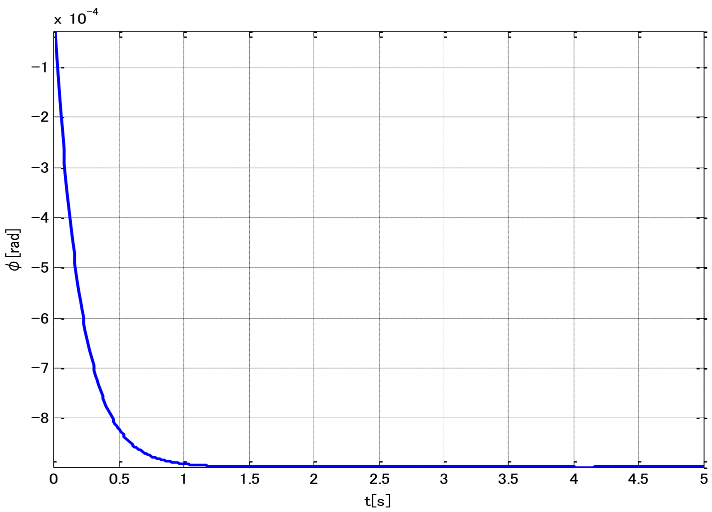

Fig.3.16 Time response of angle of deflection of the Timoshenko arm.

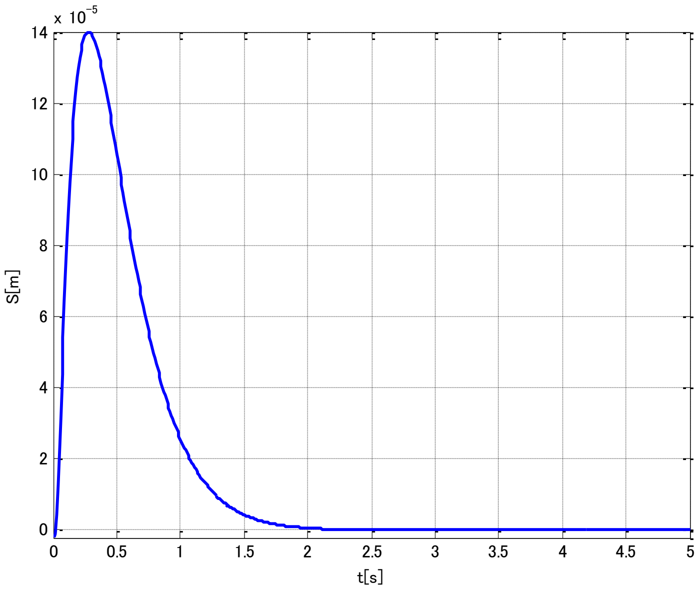

Fig.3.17 Time response of the slider position.

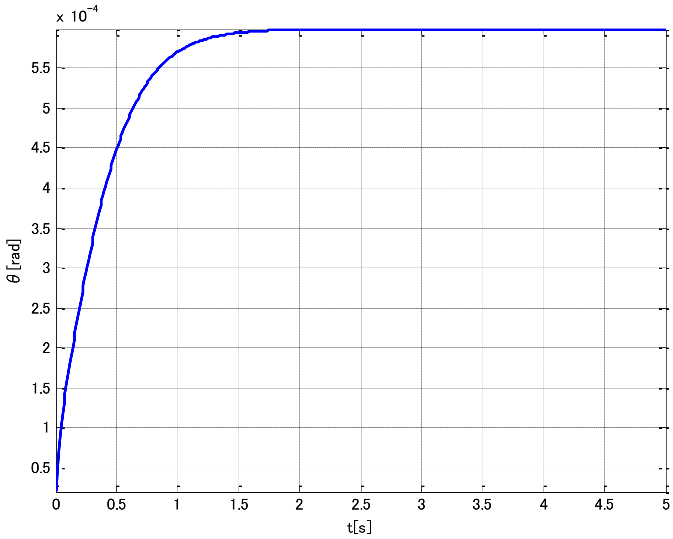

Fig.3.18 Time response of rotational angle.

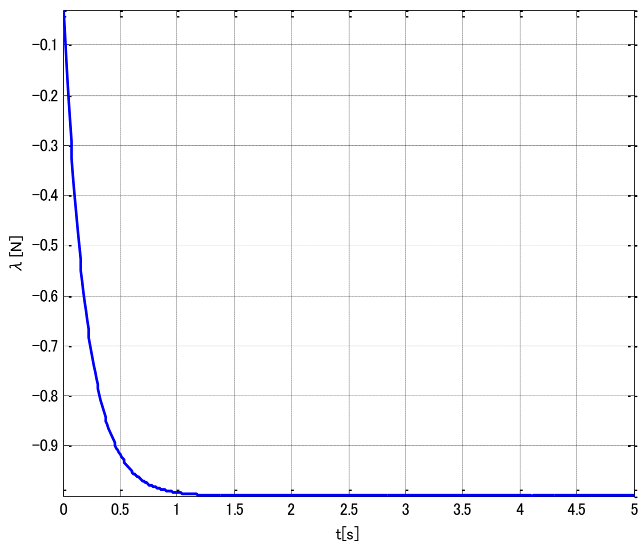

Fig.3.19 Time response of the contact force.

4. CONCLUSION

The influence of shear deformation and rotational inertia, which varies depending on the cross-sectional shape of a beam, on the result in the contact force control are examined on a one link Flexible Bernoulli-Euler Arm and one link Flexible Timoshenko. Based on the examination, we compared control object models within the range where the effects of shear deformation and rotational inertia can be ignored and verified the mechanism.

Regarding the effectiveness of beam theory, we found several features in comparison with various parameters. As a result, it was revealed that there is a range of cross sectional shape with little problem in neglecting the influence of shear deformation and rotational inertia by using Bernoulli - Euler beam theory. Timoshenko beam theory exhibited computational complexity and took a lot of time to simulate. Thus, for rotational inertia within a negligible range, simulation with Bernoulli-Euler beam theory is recommended.

Moreover, in this paper, we could only show qualitatively the characteristics in the cross-section of the beam. However, a certain rule was found in the feature. Future work in this front, we endeavor to determine quantitively the effective range of beam theory as a value by putting the thickness, width and length of the beam in a certain formula.

REFERENCES

Endo Takahiro, K. H. (2013). Force Control and Exponential Stabilization of One-Link Flexible Arm. *International Journal of Control, 87*(9), 1794-1807.

Hideo, S. (2004). *Industrial Fundamental Vibration Study.* Nishi Kendo Co., Ltd.

Hosono, T. (1984). *High-speed Laplace transform by BASIC.* Kyoritsu Publishing Co. Ltd.

Minoru Sasaki, K. N. (2015). End Point Force Control of a Flexible Timoshenko Arm. *Journal of Computer and Communications, 3*(11), 106-112.

Minoru Sasaki, T. U. (2012). Passivity-Based Control of Rotational and Translational Timoshenko Arms. *Hindawi Publishing Corporation Advances in Acoustics and Vibration, 12*, 1-6.

Shimizumi Yoshimi, M. S. (2008). Hand Position Control of a Two-DOF Planar Flexible Manipulator Based on Extension of Dynamics. *Proceedings of Measurement Automatic Control Society, 44*(5), 389-395.

Takahiro Endo, M. S. (2017). Contact-Force Control of a Flexible Timoshenko Arm. *IEEE Transaction of Autimatic Control*, *62*(2), 1004-1009.

Takahiro Endo, M. S. (2017). Contact-Force Control of a Flexible Timoshenko Arm in Rigid/Soft Environment. *IEEE Transaction of Automatic Control*, *62*(5), 2546-2553.